

# Amplitude and Frequency Modulations with Cellular Neural Networks

Baran Tander · Atilla Özmen

Published online: 1 February 2014  
© Springer Science+Business Media New York 2014

**Abstract** Amplitude and frequency modulations are still the most popular modulation techniques in data transmission at telecommunication systems such as radio and television broadcasting, gsm etc. However, the architectures of these individual systems are totally different. In this paper, it is shown that a cellular neural network with an opposite—sign template, can behave either as an amplitude or a frequency modulator. Firstly, a brief information about these networks is given and then, the amplitude and frequency surfaces of the generated quasi-sine oscillations are sketched with respect to various values of their cloning templates. Secondly it is proved that any of these types of modulations can be performed by only varying the template components without ever changing their structure. Finally a circuit is designed, simulations are presented and performance of the proposed system is evaluated. The main contribution of this work is to show that both amplitude and frequency modulations can be realized under the same architecture with a simple technique, specifically by treating the input signals as template components.

**Keywords** Cellular neural networks · Nonlinear differential equations · Amplitude modulation · Frequency modulation · Circuit design

## 1 Introduction

### 1.1 Cellular Neural Networks

Cellular neural network (CNN) is a class of dynamical neural network which was first proposed by Chua and Yang [1] and generally employed in image processing applications [2]. A

---

B. Tander  
Kadir Has Vocational School, Kadir Has University, 34590 Silivri, Istanbul, Turkey  
e-mail: tander@khas.edu.tr

A. Özmen (✉)  
Faculty of Engineering and Natural Sciences, Kadir Has University, 34230-01 Fatih, Istanbul, Turkey  
e-mail: aozmen@khas.edu.tr

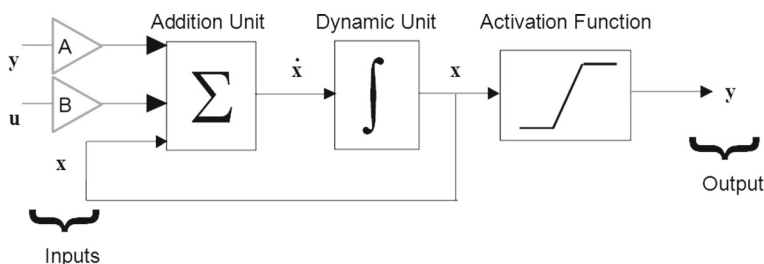


**Fig. 1** Block diagram of a CNN neuron.

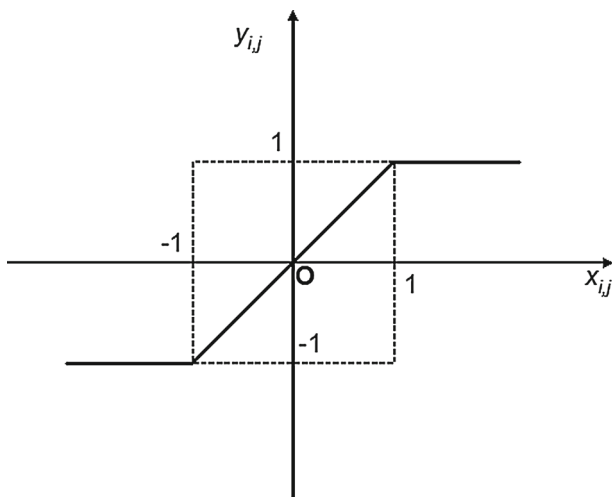


**Fig. 2** PWL activation function.

neuron (Cell) of a CNN can be modeled as seen in Fig. 1. The differential equation describing the  $C(i, j)$  cell in this structure can be written as:

$$\begin{aligned}
 -I_{i,j} + \dot{x}_{i,j} + x_{i,j} - \sum A(i, j; k, l) \cdot y_{k,l} \\
 - \sum B(i, j; k, l) \cdot u_{k,l} = 0
 \end{aligned} \quad (1)$$

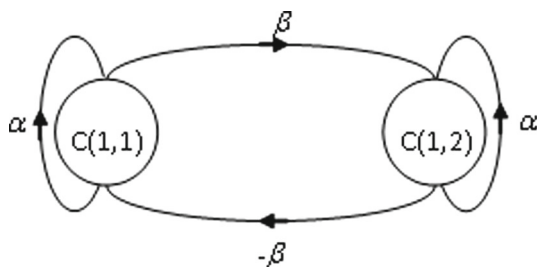
where  $x_{i,j}$  is the “state” of the cell  $C(i, j)$  which we will mostly deal throughout the paper;  $y_{k,l}$  is the “output” of its neighbor  $C(k, l)$ ;  $u_{k,l}$  is the “input” of  $C(k, l)$ ;  $A(i, j; k, l)$  is the “weight coefficient” between  $C(i, j)$  and the output of  $C(k, l)$ ;  $B(i, j; k, l)$  is another “weight coefficient” between  $C(i, j)$  and the input of  $C(k, l)$ ; and finally,  $I_{i,j}$  is a “threshold” value common for all cells. The activation function namely, “Piecewise linear function” (PWL) shown in Fig. 2 can be written as follows

$$y_{i,j} = \frac{1}{2}(|x_{i,j} + 1| - |x_{i,j} - 1|) \quad (2)$$

If we consider an  $M \times N$  – cell structure and write the above equations in matrix form, we will have:

$$\dot{x} = -x + \mathbf{A} * y(x) + \mathbf{B} * u + I \quad (3)$$

**Fig. 3** A CNN with an opposite-sign template.



The weight coefficient matrices **A** and **B** are also called “Cloning template” and “Control template” respectively. “ $*$ ” is the two-dimensional convolution operator [3]. The “Equilibrium points” are fixed values of  $x$  where the solution of (3) approaches in a stable CNN. Design process is the computation of **A**, **B** matrices and  $I$  scalar.

## 1.2 CNN with an Opposite Sign Template

A “CNN with an opposite sign template” (CNN-OST) proposed by Zou and Nossek [4] is one of the the simplest CNN structures only consists of two neurons as seen in Fig. 3. The system contains neither control templates nor threshold.

The nonlinear differential equations written in the matrix form that define the system is given below:

$$\begin{bmatrix} \dot{x}_1 \\ \dot{x}_2 \end{bmatrix} = - \begin{bmatrix} x_1 \\ x_2 \end{bmatrix} + \underbrace{\begin{bmatrix} \alpha & -\beta \\ \beta & \alpha \end{bmatrix}}_A \cdot \begin{bmatrix} y(x_1) \\ y(x_2) \end{bmatrix}; \alpha > 0; \beta > 0 \quad (4)$$

Since  $A_{12} = -A_{21}$ , the matrix is called an “Opposite-sign template”.

The paper is organized as follows: first, the oscillation constraints for the solutions of (4) are introduced and under these constraints, the amplitude and frequency surfaces of the oscillations with respect to template components are sketched. Then realizations of amplitude and frequency modulations inspired from the surfaces are explained. A circuit is proposed and simulation examples exhibiting the mentioned technique is presented. Finally at the conclusion section, the advantages and drawbacks of the CNN based AM/FM modulators are discussed.

## 2 Amplitude and Frequency Surfaces

### 2.1 Oscillation Constraint

The variations in the cloning template **A**, changes the stability of the system. Savacı and Vanderwelle [5] proved that, the  $x_1$  and  $x_2$  solutions are oscillations under the following constraint:

$$\beta > \alpha - 1 \quad (5)$$

The oscillations are quasi-sine shaped because of the nonlinear characteristic of the PWL activation function.

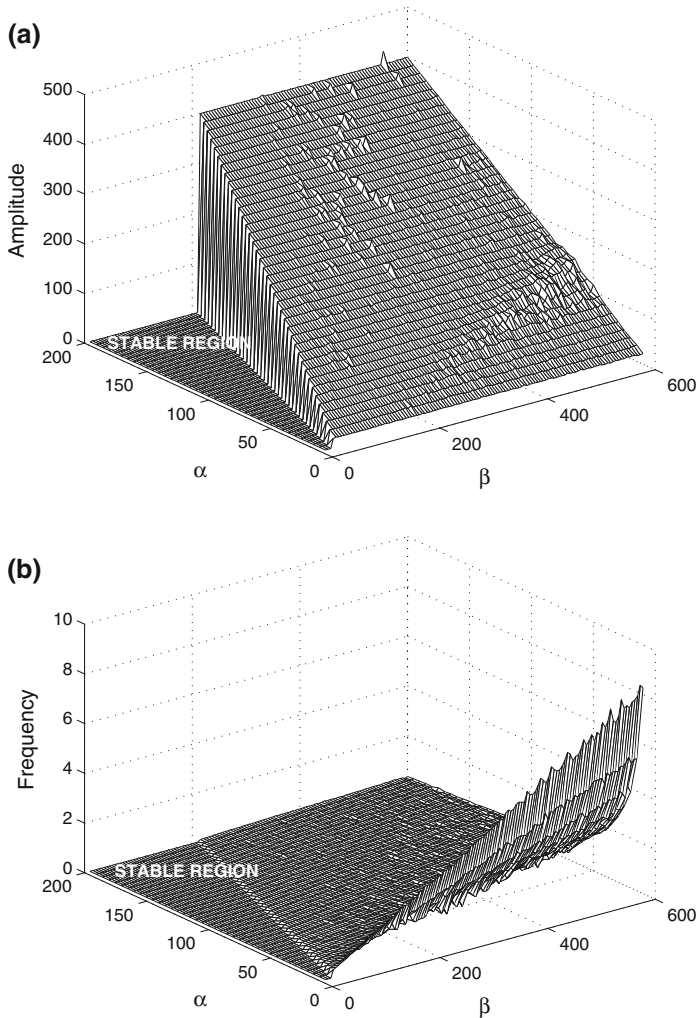


**Fig. 4** Amplitude and frequency surfaces. **a** Amplitude surface. **b** Frequency surface

## 2.2 Numerical Solution of the Equation System

In literature, there are many works related with the dynamical behaviors of CNNs [6,7]. However in our work, we dealt with the numerical solution to sketch the amplitude and frequency surfaces as functions of cloning template components  $\alpha$  and  $\beta$ . In this process, the mentioned equations in (4) are numerically solved for various values, which can be chosen in any range, somehow must satisfy the constraint given in (5). The frequencies of the oscillations are computed with the Fast Fourier Transform (FFT) of time domain solution of the equation system [8]. The two states computed in the solution set have exactly the same characteristic and waveform however with phase shifts, therefore analyzing a single state ( $x_1$ ) will be enough [9].

Amplitudes and frequencies of the solutions are evaluated and their surfaces with respect to the mentioned coefficients are sketched as shown in Fig. 4a, b. The change of amplitudes

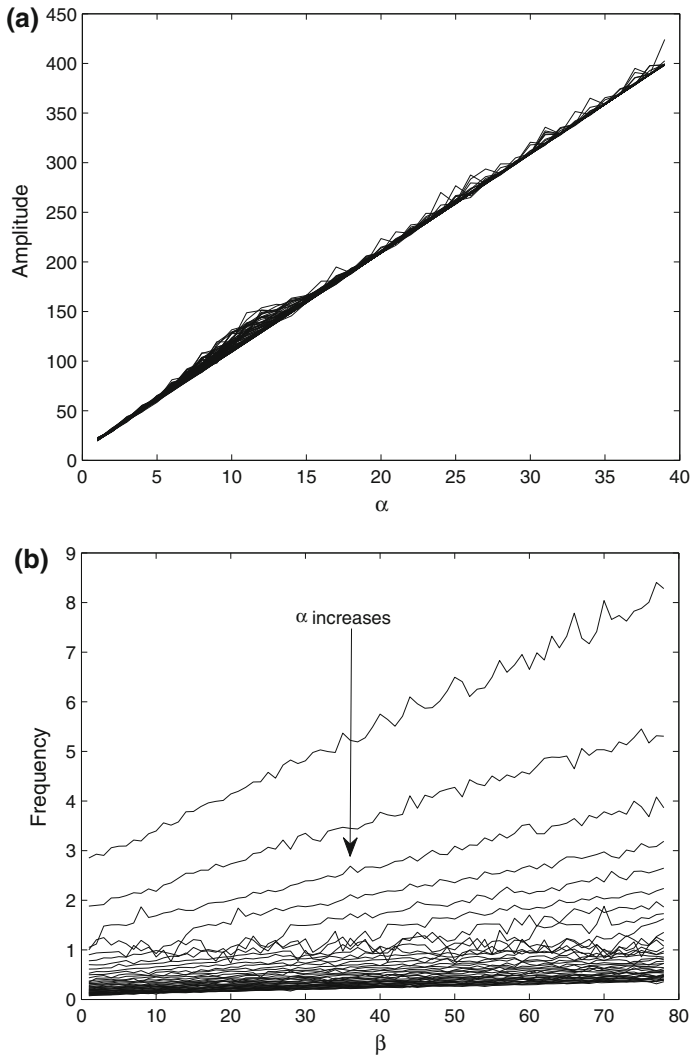


**Fig. 5** Change of amplitude and frequency. **a** Change of amplitude with  $\alpha$  for various  $\beta$  values. **b** Change of frequency with  $\beta$  for various  $\alpha$  values

and frequencies of the oscillations in two dimension are also plotted as functions of various  $\alpha$ s and  $\beta$ s in Fig. 5a, b respectively.

### 3 Amplitude and Frequency Modulation Behaviors of CNN-OST

The general process of embedding an information signal into a second signal (carrier signal) is referred to as modulation [10]. In communication systems, there are two common modulation techniques: amplitude modulation (AM) and frequency modulation (FM). In AM, the amplitude of the carrier signal is varied according to the changes in amplitude of the

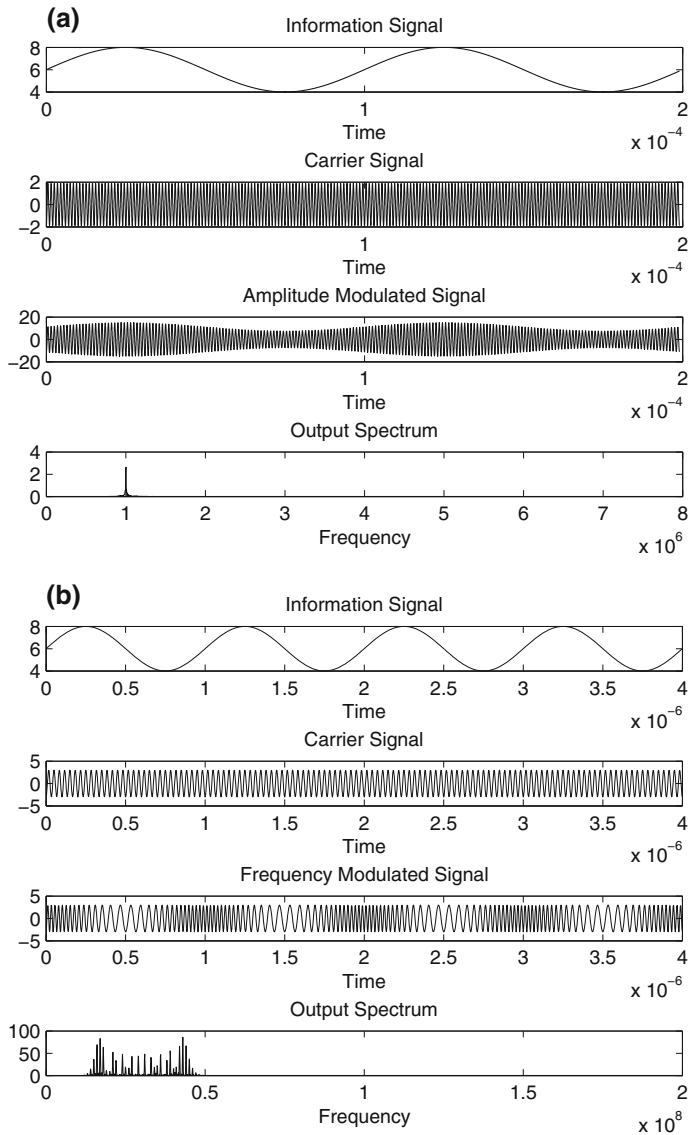


**Fig. 6** Conventional AM and FM signals. **a** Conventional AM of the information signal in (6) in time and frequency domains ( $f_c = 1,017$  kHz). **b** Conventional FM of the information signal in (6) in time and frequency domains ( $f_c = 30$  MHz).

information signal, as shown in Fig. 6a. On the other hand, in FM, the frequency of the carrier signal is varied according to the changes in amplitude of the information signal. The following sinusoidal function can be used to demonstrate AM and FM processes as seen in the Fig. 6a, b.

$$\alpha(t), \beta(t) = 6 + 2 \sin(2\pi f_0 t) \quad (6)$$

Here, the information signal's frequency  $f_0 = 10$  kHz, having a carrier frequency of  $f_c = 1017$  kHz and  $f_0 = 1$  MHz, with a carrier frequency of  $f_c = 30$  MHz are chosen for AM

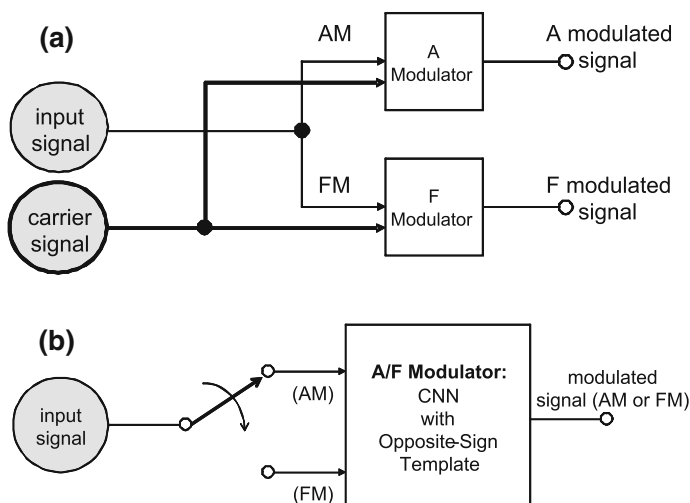


**Fig. 7** Block diagrams of the conventional and proposed amplitude and frequency modulators. **a** Conventional modulator. **b** Proposed modulator.

and FM operations respectively. FFT technique can be utilized to show both modulations' frequency domain behaviors which are presented in the mentioned figures.

In this section it is shown that, a CNN-OST is capable of performing both AM and FM without any modifications in its topology [11]. By only changing the appropriate template coefficients, the system will behave either as an AM or an FM, however, two different blocks are needed in the conventional modulators as shown in Fig. 7a, b. Moreover, no extra carrier signal besides the information signal is needed in the proposed system, since the CNN-OST can generate its own oscillations as depicted at Sect. 2.1 which indeed act as the carrier.

### 3.1 AM with CNN-OST

From the graphics in Figs. 4a and 5a, one can see that, the amplitude linearly increases with  $\alpha$  and is independent from  $\beta$ . Therefore, the variations in this coefficient, will cause a linear change in the amplitude of the  $x_{i,j}$  states. It is clear that, instead of a fixed  $\alpha$  value, if a function is chosen, the mentioned states will be the AM of this function. The matrix form of the equation that defines this case will be as follows,

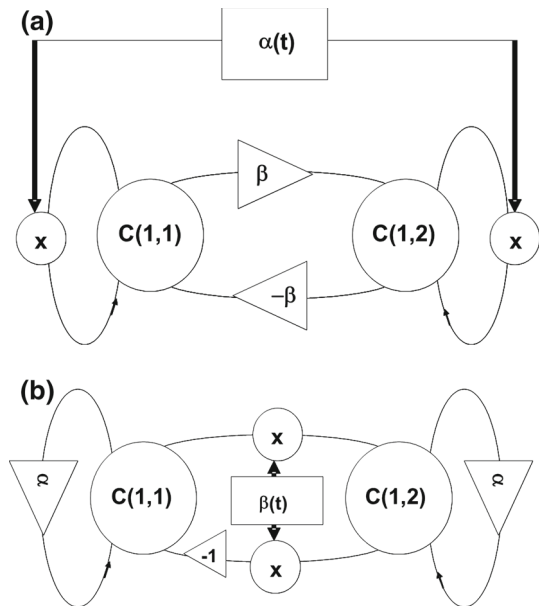
$$\begin{bmatrix} \dot{x}_1 \\ \dot{x}_2 \end{bmatrix} = - \begin{bmatrix} x_1 \\ x_2 \end{bmatrix} + \begin{bmatrix} \alpha(t) & -\beta \\ \beta & \alpha(t) \end{bmatrix} \cdot \begin{bmatrix} y(x_1) \\ y(x_2) \end{bmatrix} \quad (7)$$

Although the amplitudes are independent from  $\beta$ s, those coefficients can be used to determine the “Normalized frequency” of the carrier signal which can be chosen from the mesh in Fig. 4b. It is clear that, if modulation signals with higher frequencies are considered, the carrier's frequency must be increased by the increment of  $\beta$  or the denormalization factor  $D$ , that will be discussed at Sect. 3.3. As mentioned above, the numerical solution of (7) appears to be the AM of the signal  $\alpha(t)$ . This operation is given in Fig. 8a.

### 3.2 FM with CNN-OST

It can also be seen by the interpretation of the graphics in Figs. 4b and 5b, the frequency is proportional with  $\beta$ . Therefore, the system will act like a voltage/frequency converter

**Fig. 8** AM and FM operation of the CNN with an opposite-sign template. **a** AM operation of the CNN with an opposite-sign template, where  $\alpha(t)$  is the input with constant  $\beta$ . **b** FM operation of the CNN with an opposite-sign template, where  $\beta(t)$  is the input with constant  $\alpha$



if the  $\beta$  coefficients are applied as voltages. This means, the variations in the mentioned coefficient will change the frequency of the oscillations. Just like in Sect. 3.1, if a function is chosen instead of a constant value, the  $x_{i,j}$  states will act as the frequency modulated signal. Therefore, the solution of the below differential equation will be the FM of  $\beta(t)$ .

$$\begin{bmatrix} \dot{x}_1 \\ \dot{x}_2 \end{bmatrix} = - \begin{bmatrix} x_1 \\ x_2 \end{bmatrix} + \begin{bmatrix} \alpha & -\beta(t) \\ \beta(t) & \alpha \end{bmatrix} \cdot \begin{bmatrix} y(x_1) \\ y(x_2) \end{bmatrix} \quad (8)$$

The offset of  $\beta(t)$  will determine the central normalized frequency for FM as usual. The fixed  $\alpha$  values can be used to set the amplitude of the modulated signal and can be chosen from the mesh in Fig. 4a. Figure 8b shows the FM portion of the proposed system.

### 3.3 Operation Ranges and Denormalization

If the mesh in Fig. 4b is analyzed it will be seen that, small values of  $\alpha$  will cause a frequency shift in the amplitude modulated signal. This drawback can be minimized by choosing greater  $\alpha$ s, or by increasing the offset. However, the frequency remains constant for these greater  $\alpha$  values as seen from Fig. 5b preventing a successive FM operation. Nevertheless,  $\alpha$ s can be optimized by trial and error.

Moreover, the maximum value of the  $\alpha$ s shouldn't exceed the  $\beta$ s in any time in order to satisfy the oscillation condition given in (5). Therefore, the following constraints are essential for the amplitude and frequency modulations:

$$\begin{aligned} AM : \max[\alpha(t)] &< \beta + 1; \\ FM : \min[\beta(t)] &> \alpha - 1; \end{aligned} \quad (9)$$

Another feature of the proposed system is that, the operation at any frequency band, which is only limited by the cut-off frequencies of the components at the CNN circuit, is possible



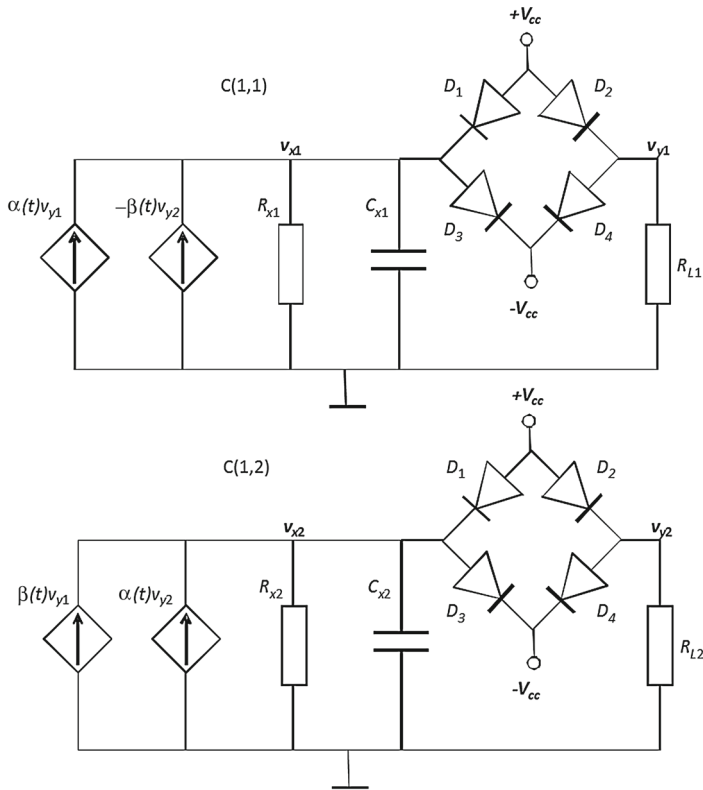


**Fig. 9** Circuit equivalent of a CNN based amplitude and frequency modulator.

with a denormalization procedure. In order to do that, a denormalization factor  $D$  must be defined. By multiplying the right hand side of the Eqs. (7) and (8) with  $D$ , the frequency will be shifted, without causing any effect to its behavior therefore, the AM and FM of the signals with much higher frequencies will be possible [12]. The denormalized equations in matrix form is given below:

$$\begin{bmatrix} \dot{x}_1 \\ \dot{x}_2 \end{bmatrix} = - \begin{bmatrix} D \cdot x_1 \\ D \cdot x_2 \end{bmatrix} + \begin{bmatrix} D \cdot \alpha(t) & -D \cdot \beta(t) \\ D \cdot \beta(t) & D \cdot \alpha(t) \end{bmatrix} \cdot \begin{bmatrix} y(x_1) \\ y(x_2) \end{bmatrix} \quad (10)$$

The following 2-step design algorithm can be used for this purpose:

- 1) Determine the normalized frequencies by interpreting Fig. 4b,  
For AM: by choosing the desired value for  $\beta$ ,  
For FM: by setting the offset value of the information signal  $\beta(t)$ ,
- 2) Shift the normalized frequencies to the operation band with the appropriate denormalization factor  $D$ .

#### 4 Circuit Equivalent of CNN-OST

One of the major advantages of CNNs is their easy implementations since the architecture requires small number of cells and weight coefficients. The topology proposed in Fig. 9, in

which the  $\alpha$  and  $\beta$  cloning template components are represented by the conductances of the voltage controlled current sources at the addition units, is suitable for the realization of the equation system at (4) [13–15]. The PWL activation function is realized by the diode bridge clipper at each cell. The  $R_x - C_x$  pair represents the dynamic unit.

The node-voltage-equation for the dynamic unit can be written as follows, where  $v_{x1}$  is the state of this cell,  $v_{y1}$  is its output and  $v_{y2}$  is the output of the neighboring cell.

$$\dot{v}_{x1} = \frac{1}{R_x C_x} (-v_{x1} + \alpha v_{y1} - \beta v_{y2}) \quad (11)$$

By choosing appropriate circuit component values, the above becomes the first row in (4). One can see that the  $\frac{1}{R_x C_x}$  coefficient is the denormalization factor  $D$ . If time dependent functions  $\alpha(t)$  and  $\beta(t)$  are chosen instead of fixed values of  $\alpha$  and  $\beta$ , the  $v_x$  state voltages will act as the AM and FM outputs. If  $R_x$  resistance is assumed to be constant, the below expression can be employed to determine the  $C_x$  capacitance for the desired operation frequency.

$$C_x = \frac{\text{Normalized Frequency}}{R_x \cdot \text{Desired Operation Frequency}} \quad (12)$$

## 5 Simulations

Simulations for various scenarios are presented to evaluate the performance of the method. The function given in (6), with an offset of 6 V and an amplitude of 2 V, having a frequency of 10 kHz for AM and 1 MHz for FM, is chosen as the information signal for the sake of comparison of the proposed method with the conventional modulation techniques given in Fig. 6a, b.

### 5.1 AM Scenario

For AM, the  $\beta$  value is chosen as 20, corresponding to an approximate carrier frequency of 0.330 Hz for the 6 V offset value of  $\alpha(t)$  which is the normalized frequency value for  $D = 1$ , where  $R_x = 1 \Omega$ ,  $C_x = 1$  F. The denormalization factor  $D$  is found as 3081.818 kHz to make the carrier frequency 1017 kHz, which belongs to one of the medium-wave national radio broadcasts in Turkey (medium frequency band: MF in radio spectrum), by selecting the  $C_x$  capacitor 0.324  $\mu$ F and  $R_x$  resistor as 1  $\Omega$  according to (12) and the design algorithm depicted at Sect. 3.3. The above sinusoidal information signal is applied as  $\alpha(t)$  and the circuit simulation results both in time and frequency domains are presented in Fig. 10a, b.

From Fig. 10b, one can see that, because of the quasi-sine shape of the carrier as well as the frequency shift depicted at Sect. 3.3., there will be side harmonics which don't exist in conventional AM operation. However this drawback won't change the shape of the recovered signal at the receiver after the demodulation process.

### 5.2 FM Scenario

It is obvious that, if the information signal's frequency is much more less than the carrier frequency in FM operation, the frequency variations at the modulated signal will be difficult to observe at time domain. Therefore, selection of an information signal with a frequency of 1 MHz is will be convenient.

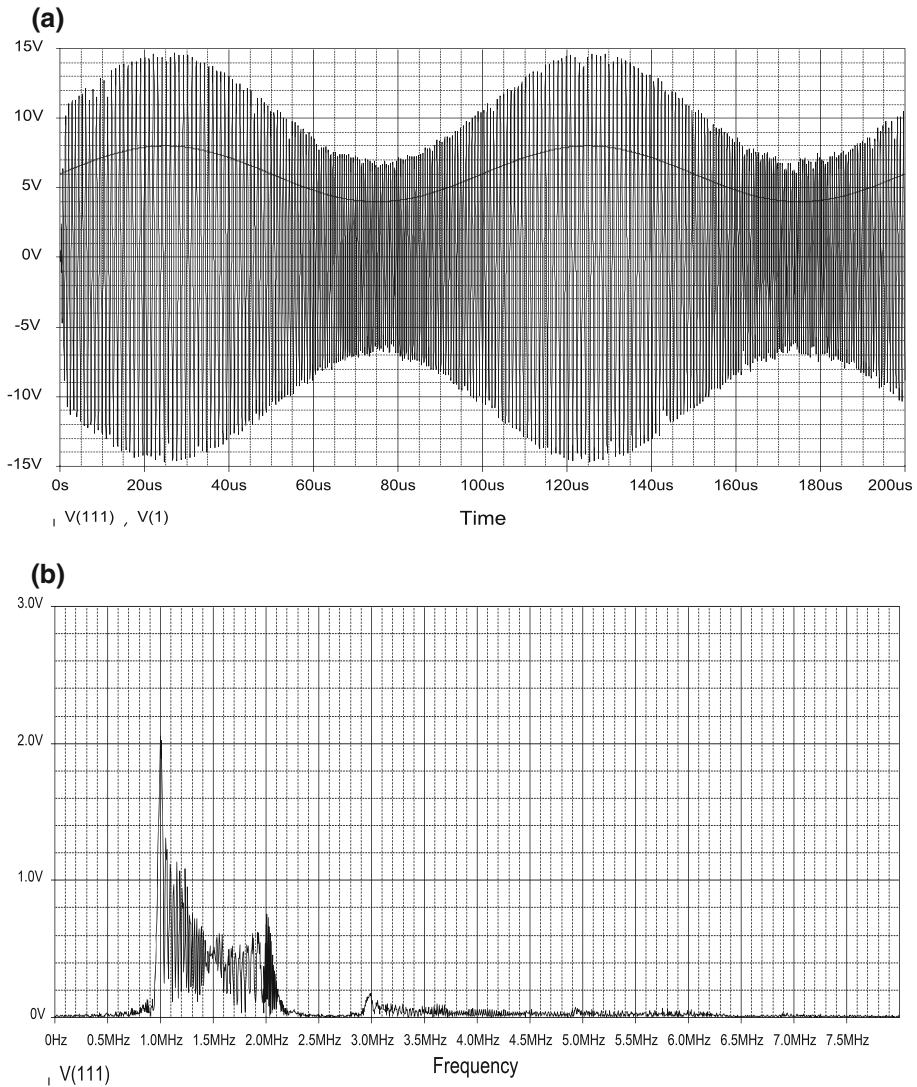


**Fig. 10** AM circuit simulation, when  $f_0 = 10$  kHz if the carrier frequency is 1017 kHz. ( $D = 3081.818$  kHz). **a** In time domain. **b** In frequency domain

Now,  $\alpha$  is fixed to 2, corresponding to an approximate carrier amplitude of 3 V. The 6 V offset of the above signal will provide an approximate normalized frequency of 0.425 Hz, if we simulate the circuit when  $D = 1$  by assuming  $R_x = 1 \Omega$  and  $C_x = 1$  F. Then,  $D = 70588.235$  kHz is introduced to shift the operation frequency to 30 MHz which belongs to very high frequency (VHF) Band in radio spectrum. In this case,  $C_x$  will be found as 14.16 nF from (12), if  $R_x = 1 \Omega$ . The time and frequency domain results observed are sketched at Fig. 11a, b.

The numerical solutions for the Eqs. (7) and (8) for the values given above, which represents the ideal characteristics of CNN based AM and FM processes are also given in Figs. 12 and 13.

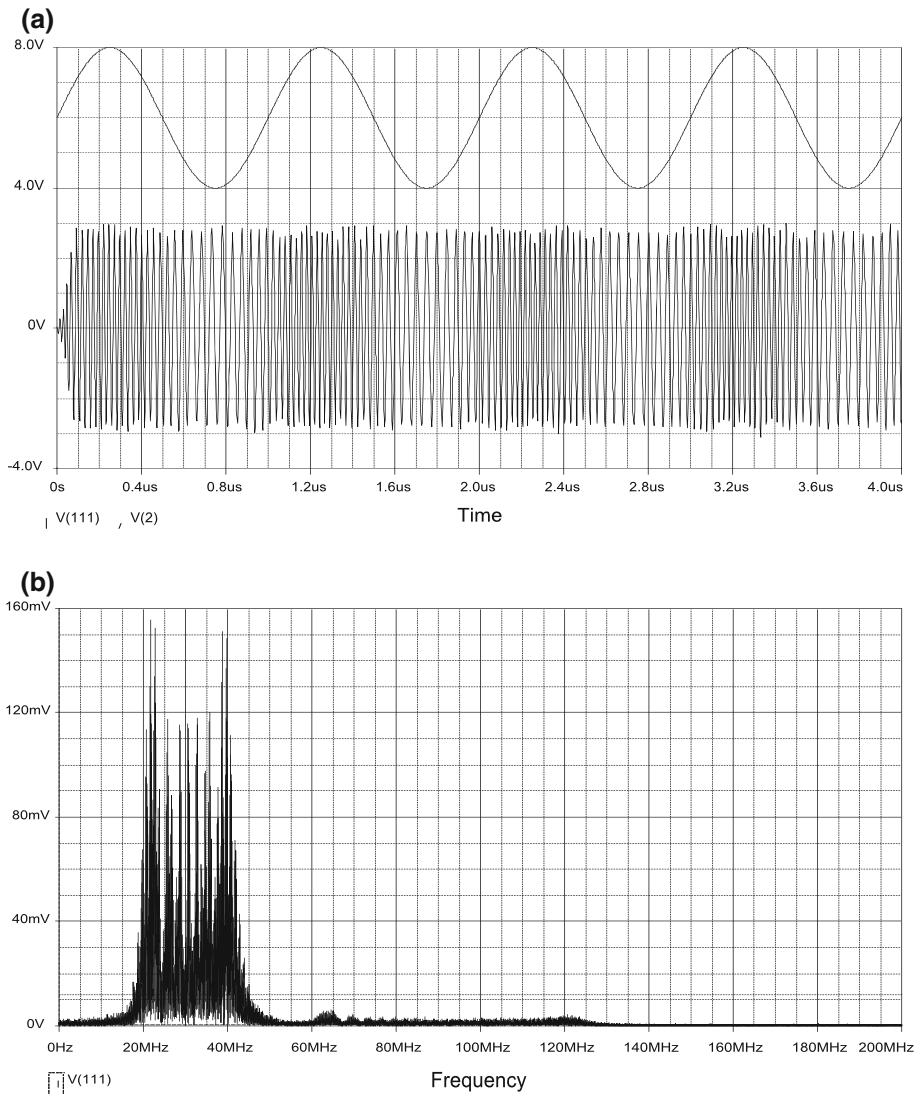


**Fig. 11** FM Circuit simulation in frequency domain, when  $f_0 = 1$  MHz if the carrier frequency is 30 MHz. ( $D = 70588.235$  kHz). **a** In time domain. **b** In frequency domain

### 5.3 Frequency Allocations

The frequency bands that are allowed for AM seem to be exceeded in praxis [16], however this is due to high amplitude of the information signal which is chosen to monitor the amplitude and frequency changes effectively in time domain. One can see that, decreasing the amplitude of the information signal -therefore the amplitude and frequency variations will be relatively less-; or choosing greater  $\alpha$  values -which will reduce the frequency sensitivity to the amplitude as seen from Fig. 5b, will minimize the interference of the harmonics with the adjacent channels at broadcast. Nevertheless, this allocations won't have any sense for personal communication applications in AM band due to empty channels.

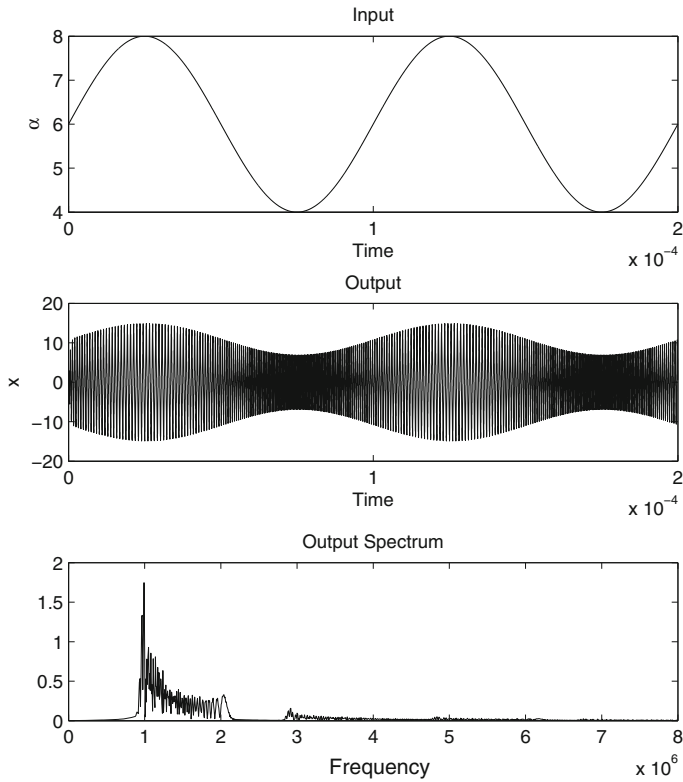


**Fig. 12** CNN based AM simulation in time and frequency domains: numerical solution of (7) when  $f_0 = 10$  kHz and with a carrier frequency of 1017 kHz ( $D = 3081.818$  kHz).

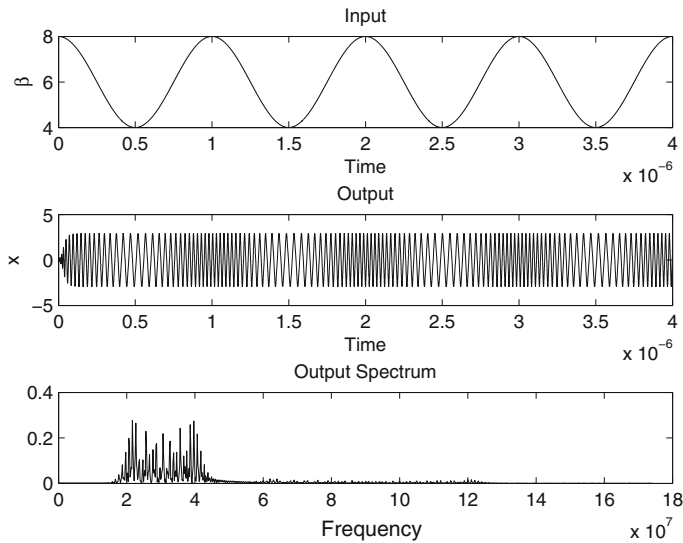


**Fig. 13** CNN based FM simulation in time and frequency domains: Numerical solution of (8) when  $f_0 = 1$  MHz and with a carrier frequency of 30 MHz ( $D = 70588.235$  kHz).

## 6 Conclusions

In this paper, it is shown that one adaptive system depending on a special architecture is sufficient to perform both amplitude and frequency modulations. The system depends on the numerical solution of nonlinear differential equations defining a simple CNN structure called CNN-OST.

Since a single circuit is employed instead of two individual circuits for two different modulations, it is clear that the number of components therefore the cost of the system will be relatively less. The drawbacks of using a CNN for the modulations is that, the waveform of the carrier signal is not an exact sinewave because of the effect of PWL activation functions in the neurons, as well as a possible violations at AM band in praxis. Nevertheless, the proposed technique is believed to be useful in many applications.

## References

1. Chua LO, Yang L (1988) Cellular neural networks: theory. *IEEE Trans Circuit Syst* 35:1257–1272
2. Costantini G, Casali D, Carota M (2005) Detection of moving objects in 2-D images based on a CNN algorithm and density based spatial clustering. *WSEAS Trans Circuits Syst* 4:440–447
3. Gonzales RC, Woods RE (2008) Digital image processing, 3rd edn. Prentice Hall, Upper Saddle River
4. Zou F, Nossek JA (1991) Stability of cellular neural networks with opposite-sign templates. *IEEE Trans Circuits Syst* 38:675–677
5. Savaci FA, Vanderwalle J (1993) On the stability of cellular neural networks. *IEEE Trans CAS- I: Fund Theo Apps* 40:213–215
6. Pana L, Cao J (2011) Anti-periodic solution for delayed cellular neural networks with impulsive effects. *Nonlinear Anal Series B* 12(6):3014–3027
7. Song Q, Cao J (2008) Dynamical behaviors of discrete-time fuzzy cellular neural networks with variable delays and impulses. *J Franklin Inst* 345(1):39–59
8. Özmen A, Tander B (2006) A numerical method for frequency determination in the astable cellular neural networks with opposite-sign templates. *SIU'06 IEEE 14th Signal Processing and Communication Application Symposium*, Antalya, Turkey
9. Tander B, Ün M (2000) Generalized PSPICE and SIMULINK models for the continuous-time simulations of cellular neural networks. *BCSP'00, 1st IEEE Balkan Conference on Signal Processing, Communications, Circuits and Systems*, Istanbul, Turkey
10. Oppenheim AV, Willsky AS, Nawab H (1997) Signals and systems, 2nd edn. Prentice Hall, Upper Saddle River
11. Tander B, Özmen A (2012) Amplitude and frequency modulation behaviours of cellular neural networks. *INISTA'2012: The 6th International Symposium on Innovations in Intelligent Systems and Applications*, Trabzon, Turkey
12. Tander B, Baskan M, Senol C (2002) Experimental analysis of transients in small scaled cellular neural networks. *ELECO'02: 4th Electrical, Electronics, Computer Engineering Symposium*, Bursa, Turkey
13. Tander B, Ün M (2000) Diode Bridge Clipper as an activation function circuit at the PSPICE simulations of cellular neural networks. *ELECO'00: 2nd Electrical, Electronics, Computer Engineering Symposium*, Bursa, Turkey
14. Tander B, Özmen A, Özcelep Y, Design and implementation of a cellular neural network based oscillator circuit. *CSECS'2009 The 8th WSEAS International Conference on Recent Advances in Circuits, Systems, Electronics, Control and Signal Processing*, Tenerife, Spain
15. Tander B, Özmen A, Özcelep Y (2010) Design and implementation of a negative feedback oscillator circuit based on a cellular neural network with an opposite sign template. *WSEAS Trans Circuits Syst* 9:60–69
16. FCC: Federal Communications Commission Office of Engineering and Technology Policy and Rules Division, FCC Online Table of Frequency Allocations, 47 C.F.R. 2.106, 2010